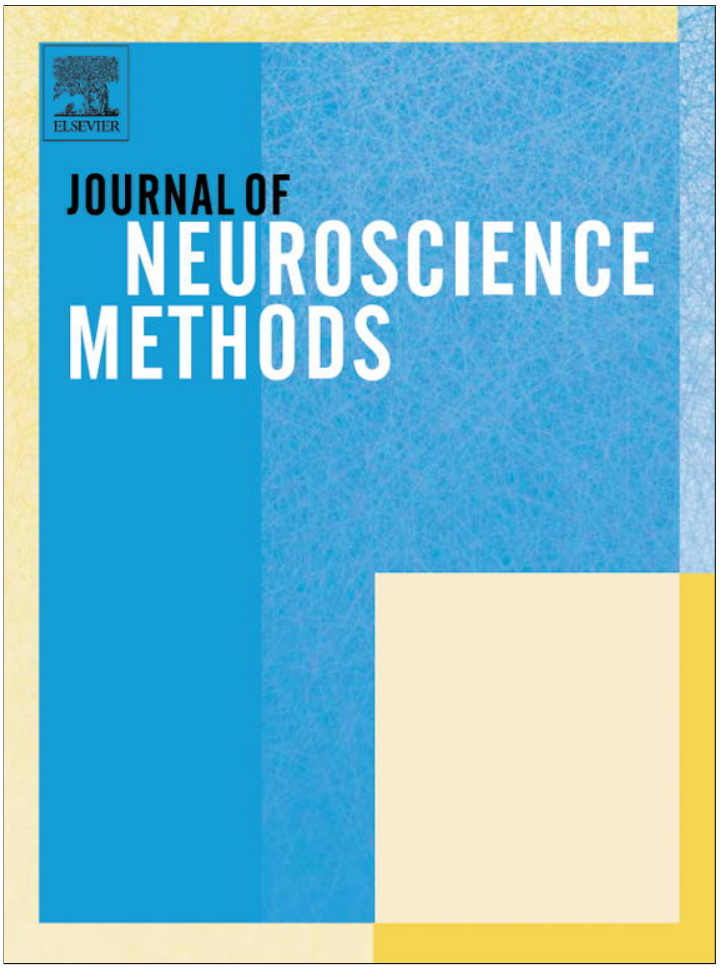

Journal of Neuroscience Methods 216 (2013) 142–145

Contents lists available at SciVerse ScienceDirect

Journal of Neuroscience Methods

journal homepage: www.elsevier.com/locate/jneumeth

Basic Neuroscience

Photoacoustic and optical coherence tomography of epilepsy with high temporal and spatial resolution and dual optical contrasts

Vassiliy Tsytsarev[a,b,1,2], Bin Rao[a,1,3], Konstantin I. Maslov[a,1,3], Li Li[a,c,4], Lihong V. Wang[a,*]

[a] Optical Imaging Laboratory, Department of Biomedical Engineering, Washington University in St. Louis, One Brookings Drive, St. Louis, MO 63130, United States
[b] University of Maryland School of Medicine, Department of Anatomy and Neurobiology, 20 Penn Street, HSF-II, Baltimore, MD 22201, United States
[c] Massachusetts General Hospital, Harvard Medical School, Wellman Center for Photomedicine, 40 Parkman Street, Room 160, Ruth Sleeper Hall, Boston, MA 02114, United States

HIGHLIGHTS

- Epileptic seizures in the mice neocortex were induced *in vivo* by intracortical injection of 4-aminopyridine.
- Optical coherence tomography and photoacoustic images of the cortex were acquired simultaneously.
- We have observed a decrease in optical scattering caused by the epileptic seizures.
- We have observed vasodilatation of the small blood caused by the epileptic seizures.

ARTICLE INFO

Article history:
Received 28 January 2013
Received in revised form 1 April 2013
Accepted 4 April 2013

Keywords:
Photoacoustic microscopy
Optical coherence tomography
Epileptic seizures
4-Aminopyridine

ABSTRACT

Epilepsy mapping with high spatial and temporal resolution has great significance for both fundamental research on epileptic neurons and the clinical management of epilepsy. In this communication, we demonstrate for the first time *in vivo* epilepsy mapping with high spatial and temporal resolution and dual optical contrasts in an animal model. Through the variations of a depthresolved optical coherence tomography signal with optical scattering contrast, we observed that epileptic neuron activities modulated the optical refractive index of epileptic neurons and their surrounding tissue. Simultaneously, through neurovasculature coupling mechanisms and optical absorption contrast, we used photoacoustic signals to document the hemodynamic changes of the microvasculature surrounding the epileptic neurons. The epilepsy mapping results were confirmed by a simultaneously recorded electroencephalogram signal during epileptic seizure. Our new epilepsy mapping tool, with high temporal and spatial resolution and dual optical contrasts, may find many applications, such as drug development and epilepsy surgery.

1. Introduction

Epilepsy results from "electrical storms" inside the brain that cause recurring seizures. About 2 in 100 people in the United States experience an unprovoked seizure at least once in their lives. The population and shape of involved epileptic neurons vary along the time course of each epileptiform event in a very short time span (Pinto et al., 2011). Current clinical functional imaging methods, such as functional magnetic resonance imaging (fMRI) (Lin and Chiang, 2013), positron emission tomography (PET) and single-photon emission computed tomography (SPECT), are limited by their low temporal resolution in documenting such paroxysmal epileptiform events (Craven et al., 2010). High temporal resolution is critical to overcome the motion artifacts caused by patients or procedures during epilepsy surgery. Although optical mapping methods such as intrinsic optical imaging (IOS) (Bahar et al., 2006; Inyushin et al., 2001; Haglund and Hochman, 2004; Schwartz et al., 2004; Schwartz and Bonhoeffer, 2001) and voltage-sensitive dye imaging (VSD) (Cohen and Lesher, 1986; Tsytsarev et al., 2008, 2009, 2010) have limitations in imaging depth and tissue toxicity, the development of epileptic animal models has made them very useful (Raol and Brooks-Kayal, 2012). More recent developments in the optical mapping of neural activities include the optical coherence tomography (OCT) (Satomura et al., 2004; Aguirre et al.,

* Corresponding author at: Department of Biomedical Engineering, Washington University in St. Louis, One Brookings Drive, St. Louis, MO 63130, United States. Tel.: +1 314 935 4911.
E-mail addresses: tsytsarev@umaryland.edu (V. Tsytsarev), raob@seas.wustl.edu (B. Rao), kimaslov@biomed.wustl.edu (K.I. Maslov), li.li@mgh.harvard.edu (L. Li), lhwang@seas.wustl.edu, lhwang@wustl.edu (L.V. Wang).
[1] These authors contribute equally to this manuscript.
[2] University of Maryland School of Medicine, Department of Anatomy and Neurobiology, HSF II Room S251, 20 Penn Street, Baltimore, MD 21201-1075, United States. Tel.: +1 410 706 8907.
[3] Tel.: +1 314 935 4911.
[4] Massachusetts General Hospital, Harvard Medical School, Wellman Center for Photomedicine, 40 Parkman Street, Room 160, Ruth Sleeper Hall, Boston, MA 02114, United States. Tel.: +1 617 643 5310.

0165-0270/$ – see front matter © 2013 Elsevier B.V. All rights reserved.
http://dx.doi.org/10.1016/j.jneumeth.2013.04.001

2006; Rajagopalan and Tanifuji, 2007; Chen et al., 2009; Sato et al., 2010; Liang et al., 2011; Lenkov et al., 2005; Eberle et al., 2012) and photoacoustic microscopy (PAM) (Hu et al., 2009; Maslov et al., 2008; Tsytsarev et al., 2011; Wang et al., 2003; Wang, 2008, 2009; Liao et al., 2010, 2012a, 2012b; Yao et al., 2012). OCT can image both the refractive index modulation of the tissue that surrounds epileptic neurons with optical scattering contrast and the neuron-vasculature coupled blood flow patterns with Doppler OCT contrast. PAM represents an innovation in the functional imaging of red blood cells and blood flow. It provides functional data such as the oxygen saturation of red blood cells in the microvasculature. Because PAM is based on pure optical absorption contrast, it does not require the dense optical scans required by Doppler OCT, and it is immune to axial motion artifacts that may significantly compromise the blood flow images generated by the Doppler OCT in *in vivo* applications. As a rapidly evolving imaging technology, PAM promises deep imaging into tissue due to its multi-scale imaging capability (Wang and Hu, 2012; Tsytsarev et al., 2012a,b). By recording the optical refractive index modulation with OCT technology and simultaneously documenting the hemodynamic changes in epileptiform events with PAM, we can, for the first time, perform epilepsy mapping with high temporal and spatial resolution and dual optical contrasts. We expect our demonstrated technology to have great utility in applications such as epilepsy drug development and epilepsy surgery.

2. Materials and methods

2.1. Animal preparations

For each experiment, a Swiss Webster mouse (Hsd: ND4, 25–30 g; Harlan, Indianapolis, IN) was anesthetized by an intraperitoneal (IP) injection of a mixture of ketamine (87 mg/kg) and xylazine (13 mg/kg). The anaesthetized animal was placed in a custom-made stereotaxic head holder, and the left dorsal portion of the skull was exposed by surgically removing the scalp and muscle. A cranial opening (~4–5 mm^2) was made using a dental drill over the left hemisphere, and the exposed dura mater surface was cleaned with artificial cerebrospinal fluid (ACSF). Throughout the experiment, the animal was supplied with breathing-grade compressed air (AI B300, Airgas, MO) and maintained under anesthesia using isoflurane (1.0–1.5% with an airflow rate of ~1 L/min), while the body temperature of the animal was maintained at 37 °C by a temperature-controlled electrical heating pad. After each experiment, the animal was euthanized with an overdose of pentobarbital. All experimental animal procedures were carried out in conformance with the laboratory animal protocol approved by the Animal Studies Committee of Washington University in St. Louis.

2.2. Inducement of the epileptic seizures

After craniotomy, 0.35 μL of a 25 mM solution of 4-aminopyridine (4-AP) in artificial cerebrospinal fluid (ACSF) was injected into cortical layers II–III, using an injector device (Nanojet II) with a 15–25 μm diameter glass microcapillary (Bahar et al., 2006; Tsytsarev et al., 2012b). The injector was mounted on a micromanipulator that allowed injections 0.2–0.3 mm below the duramater surface. A single channel electroencephalogram (EEG) was recorded through a screw-type electrode placed in the left hemisphere in the skull, then amplified by an AC/DC differential amplifier (A-M Systems, Model 3000), digitized at 5000 Hz, and recorded. The start of EEG data acquisition was manually initiated.

2.3. Optical epilepsy mapping with dual contrasts

A dual modality optical imaging system that can simultaneously provide a co-registered OCT image and a PAM image (Fig. 1) was used to provide optical mappings of epilepsy. The OCT imaging channel provided depth-resolved brain tissue structure images based on optical scattering contrast (Rao et al., 2008). The PAM channel provided depth-resolved brain vasculature images based on optical absorption contrast (Rao et al., 2010a). OCT and PAM A-lines were acquired sequentially for each scanning location. Thus, an OCT image and a PAM image were recorded virtually simultaneously. Each B-scan frame contained 800 scanning points (A-lines). At an imaging speed of 5000 A-lines-per-second, 500 B-scan frames were acquired within an 80-s time window (Rao et al., 2010b). Similar to the procedures described in our previous publications (Tsytsarev et al., 2011; Hu et al., 2009), we identified two vessels close to the 4-AP injection site and performed repeated B-scans over the selected vessels to map epilepsy in both spatial and time dimensions. The temporal resolution of epilepsy mapping was 6.25 Hz. The spatial lateral resolutions of epilepsy mapping with OCT and PAM were 5.2 μm and 3.5 μm, respectively.

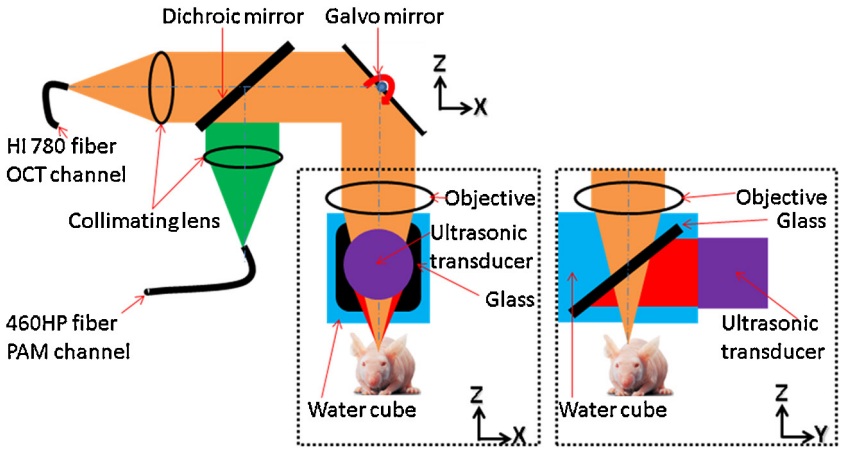

Fig. 1. Schematic of the dual-modality OCT/PAM imaging probe. The OCT system was connected to the dual-modality probe through a single-mode fiber (HI-780, Thorlabs). The 532 nm pulsed laser was connected to the probe with another single-mode fiber (460-HP, Thorlabs). The collimated OCT sample and the 532 nm PAM excitation beams were combined using a dichroic mirror and focused by a microscope objective (NA 0.1) at 200 μm below the tissue surface. Fast optical scanning along one axis (B-scan) was done by a galvanometer mirror. Upon the absorption of the laser pulse by the tissue, photoacoustic waves were generated. Thereafter, the waves were reflected by a glass plate placed at 45° between the objective and the animal, and detected by the cylindrically focused ultrasonic transducer (GE, 25 MHz bandwidth). The whole probe was attached to a one-dimensional mechanical stage, which scanned perpendicularly to the fast optical scan axis. The OCT A-line image and the PAM A-line image were acquired sequentially for each A-line.

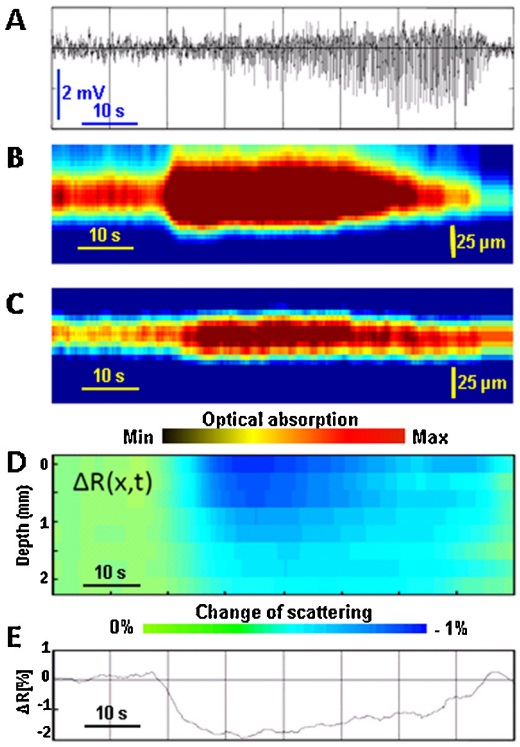

Fig. 2. Time course of an epileptic seizure development. (A) Electroencephalogram (EEG) of the epileptic seizure. (B) Plot of maximum amplitude projection (MAP) images from PAM versus time for a vein, capturing the vasodilatation process, which was well correlated with EEG signals. (C) Plot of MAP images of PAM versus time of an artery, capturing a similar vasodilatation process during seizure, but with a reduced amplitude and prolonged time. (D) Depth-resolved reflectivity change $\Delta R(x,t)$, where x represents depth and t represents time. (E) Averaged optical reflectivity change $\Delta R(t)$ of the affected brain cortex tissue, showing how it is affected by the seizure.

After image acquisition, three types of image data (EEG, OCT, PAM) were analyzed separately. The EEG data was simply displayed as voltage versus time. For the OCT data, the optical scattering signal intensity was calculated by Fourier transformation of the interference fringe recorded by a line-scan CCD camera. Using the first B-scan image as a baseline, we calculated the depth-resolved reflectivity change $\Delta R(x,t)$, where x represents depth and t represents the time or B-scan number, by averaging 800 A-lines within every B-scan image. Then, $\Delta R(x,t)$ was averaged along the imaging depth to generate an averaged reflectivity change over time, $\Delta R(x,t)$. For PAM data, the A-line amplitude of the photoacoustic signal was extracted via Hilbert transformation. The vessel diameter was directly shown by the maximum amplitude projection (MAP) of PAM B-scan images. Changes in vessel diameter could be directly visualized from the plot of MAP images along the time axis.

3. Results

After a 4-AP intracortical injection, epileptic seizures occurred periodically for 2–4 h, lasting 20–200 s at intervals of 2–20 min. Fig. 2A records a typical seizure EEG signal course lasting about 80 s. Fig. 2B and C plot the 1D vertical MAP images from PAM along the horizontal time axis. A large vasodilatation of the blood vessels (veins), as shown in Fig. 2B, signals the electrographic onset of seizure, which is well-correlated with the EEG signal. The vessel (artery) in Fig. 2C displays a similar vasodilatation effect, but with reduced amplitude and prolonged duration. It is interesting to note that significant vasodilatation occurred only near the injection site. Outside a cortical area of about 1 mm^2, vasodilatation was below our detection threshold of about 10%. Additionally, it seems that the vasodilatation may signal the beginning of seizure earlier than conventional EEG signals. From Fig. 2B, we observed that after the large vessel dilation the vessel was smaller than the baseline diameter. Further study might be interesting, but is beyond the scope of this communication.

The depth-resolved reflectivity change $\Delta R(x,t)$ during seizure is shown in Fig. 2D. From the plot of $\Delta R(x,t)$, we can easily visualize the depth-resolved reflectivity change along the whole time course of the seizure. A reflectivity change $\Delta R(t)$ averaged along the depth direction at each sampling time point can represent the trend of reflectivity variation in a simple plot, as shown in Fig. 2E. The suddenly decreased reflectivity (represented by the color change from green to blue in Fig. 2D and by the curved dip in Fig. 2E) coincided with the start of vessel dilation. The changes in cortical reflectivity ended approximately at the seizure's end. In spite of the low transparency of the brain tissue, we were able to record the tissue-scattering signal from 2 mm below the surface, which is deeper than the cortical thickness. With fair confidence, we conclude that both $\Delta R(x,t)$ and $\Delta R(t)$ are more sensitive in signaling the start and the end of the seizure than EEG signals.

4. Discussion

The 4-AP model of epileptic seizures (Bahar et al., 2006; Tsytsarev et al., 2011; Zhao et al., 2011; Raol and Brooks-Kayal, 2012) allows us to investigate periods of induction, maintenance, and propagation of seizure discharges, and has been extensively studied using different optical methods. It is generally known that epileptic seizures are accompanied by a local increase in cerebral blood flow to the epileptic focus (Zhao et al., 2011; Hirase et al., 2004; Santisakultarm and Schaffer, 2011; Schwartz et al., 2004), but the relationship between seizures and neuronal activity remains unclear. The trigger mechanism of the seizure as a synchronized activity of the neural network is also not very well established. Although it is unlikely that vasodilatation itself can initiate the seizure, fast vasodilatation might be a first indicator of the local biochemical process that accompanies the seizure's beginning. It was proposed by Pereira de Vasconcelos et al. (1995) that nitric oxide triggers vasodilation in response to focal epileptic seizures, but in their work, vasodilatation was observed in a relatively large area, including both the cortex around epileptic foci and also (bilaterally) the substantia nigra and the parafascicular thalamic nucleus. It seems possible that astrocytes' release of glutamate in the area of the epileptic foci plays a causal role in synchronous firing of a large neural population (Carmignoto and Haydon, 2012; Inyushin et al., 2010, 2012). Synchronous activity of the astrocytic syncytium can cause changes in the optical features of the cortical tissue that can be observed by OCT.

OCT has been used for *in vivo* brain imaging in animal experiments (Satomura et al., 2004; Aguirre et al., 2006; Rajagopalan and Tanifuji, 2007; Chen et al., 2009; Sato et al., 2010; Liang et al., 2011; Lenkov et al., 2005; Eberle et al., 2012) and provides high spatial resolution and a wide field of view. The modulation of the optical refractive index by the epileptic neuronal activity during a seizure coincides with the observation of surface reflectivity changes. As demonstrated in our experiments, OCT represents a very effective direct optical epilepsy mapping method, with a depth range of about 2 mm. Due to the well-known neurovasculature coupling mechanism, dynamic blood flow changes such as the vasodilatation observed in our experiments may be established as another effective optical epilepsy mapping method for documenting epilepsy seizure. Theoretically, most blood flow imaging methods, including Doppler OCT and its variants, could be used to record the dynamic blood flow change caused by an epileptic seizure. The recently invented PAM technology has major advantages due to both its high contrast (as high as 40 dB) and its multi-scale imaging capability,

which provides a much deeper imaging depth not achievable by other optical imaging technologies. In this demonstration, we used a very simple epilepsy mapping protocol, which does not utilize the full speed of our imaging systems (20,000 A-lines-per-second). It is very straightforward to upgrade the dual contrast imaging system to a 100,000 or 200,000 A-lines-per-second imaging speed, enabling more sophisticated mapping protocols. The dual contrast optical epilepsy mapping method demonstrated in this short communication presents a new tool for epilepsy drug development with small animal models (Raol and Brooks-Kayal, 2012). With appropriate modifications, it could be used as an intra-operative tool for determining the boundary of epileptic tissue in epilepsy surgery (Haglund and Hochman, 2004).

5. Conclusions

We demonstrate for the first time *in vivo* epilepsy mapping with high spatial and temporal resolution and dual optical contrasts in an animal model. Through the variations in a depth-resolved optical coherence tomography signal with optical scattering contrast, we observed variations of the depth resolved optical reflection signal from epilepsy tissue. Simultaneously, through neurovascular coupling mechanisms and optical absorption contrast, we used photoacoustic signals to document the hemodynamic changes of the microvasculature surrounding the epileptic neurons. The epilepsy mapping results were confirmed by a simultaneously recorded electroencephalogram signal during epileptic seizure. Our new epilepsy mapping tool, with high temporal and spatial resolution and dual optical contrasts, may find many applications, such as in drug development and epilepsy surgery.

Acknowledgements

This work was sponsored in part by National Institutes of Health grants R01 EB008085, R01 CA134539, U54 CA136398, R01 CA157277, R01 CA159959, DP1 EB016986 (NIH Director's Pioneer Award). L.W. has a financial interest in Microphotoacoustics, Inc. and Endra, Inc., which, however, did not support this work. K.M. has a financial interest in Microphotoacoustics, Inc., which, however, did not support this work.

References

Aguirre AD, Chen Y, Fujimoto JG, Ruvinskaya L, Devor A, Boas DA. Depth-resolved imaging of functional activation in the rat cerebral cortex using optical coherence tomography. Opt Lett 2006;31(23):3459–61.

Bahar S, Suh M, Zhao M, Schwartz TH. Intrinsic optical signal imaging of neocortical seizures: the 'epileptic dip'. Neuroreport 2006;17(5):499–503.

Carmignoto G, Haydon PG. Astrocyte calcium signaling and epilepsy. Glia 2012;60:1227–33.

Chen Y, Aguirre AD, Ruvinskaya L, Devor A, Boas DA, Fujimoto JG. Optical coherence tomography (OCT) reveals depth-resolved dynamics during functional brain activation. J Neurosci Methods 2009;30(178(1)):162–73.

Cohen LB, Lesher S. Optical monitoring of membrane potential: methods of multisite optical measurement. Opt Methods Cell Physiol 1986;40:71–99.

Craven I, Kotsarini C, Hoggard N. Recent advances in imaging epilepsy. Postgrad Med J 2010;86(1019):552–9.

Eberle M, Reynolds C, Szu J, Wang Hansen A, Hsu M, Islam M, et al. *In vivo* detection of cortical optical changes associated with seizure activity with optical coherence tomography. Biomed Opt Express 2012;3:2700–6.

Hirase H, Creso J, Buzsaki G. Capillary level imaging of local cerebral blood flow in bicuculline-induced epileptic foci. Neuroscience 2004;128(1):209–16.

Haglund MM, Hochman DW. Optical imaging of epileptiform activity in human neocortex. Epilepsia 2004;45(Suppl. 4):43–7.

Hu S, Maslov K, Tsytsarev V, Wang LV. Functional transcranial brain imaging by optical-resolution photoacoustic microscopy. J Biomed Opt 2009;14(4):040503.

Inyushin MY, Vol'nova AB, Lenkov DN. Use of a simplified method of optical recording to identify foci of maximal neuron activity in the somatosensory cortex of white rats. Neurosci Behav Physiol 2001;31(2):201–5.

Inyushin M, Kucheryavykh LY, Kucheryavykh YV, Nichols CG, Buono RJ, Ferraro TN, et al. Potassium channel activity and glutamate uptake are impaired in astrocytes of seizure-susceptible DBA/2 mice. Epilepsia 2010;51(9):1707–13.

Inyushin MY, Huertas A, Kucheryavykh YV, Kucheryavykh LY, Tsydzik V, Sanabria P, et al. L-DOPA uptake in astrocytic endfeet enwrapping blood vessels in rat brain. Parkinsons Dis 2012;2012:321406.

Lenkov DN, Volnova AB, Pope ARD, Tsytsarev V. Advantages and limitations of brain imaging methods in the research of absence epilepsy in humans and animal models. J Neurosci Methods 2005;212(2):195–202.

Liang CP, Wierwille J, Moreira T, Schwartzbauer G, Jafri MS, Tang CM, et al. A forward-imaging needle-type OCT probe for image guided stereotactic procedures. Opt Express 2011;19(27):26283–94.

Liao LD, Lin CT, Shih YY, Duong TQ, Lai HY, Wang PH, et al. Transcranial imaging of functional cerebral hemodynamic changes in single blood vessels using *in vivo* photoacoustic microscopy. J Cereb Blood Flow Metab 2012a;32(6):938–51.

Liao LD, Lin CT, Shih YY, Lai HY, Zhao WT, Duong TQ, et al. Investigation of the cerebral hemodynamic response function in single blood vessels by functional photoacoustic microscopy. J Biomed Opt 2012b;17(6):061210.

Liao LD, Li ML, Lai HY, Shih Y, Lo YC, Tsang S, et al. Imaging brain hemodynamic changes during rat forepaw electrical stimulation using functional photoacoustic microscopy. Neuroimage 2010;52(2):562–70.

Lin CH, Chiang MC. Applying magnetic resonance imaging to structural and functional brain research. J Neurosci Neuroeng 2013;2:29–37.

Maslov KI, Zhang HF, Hu S, Wang LV. Optical-resolution photoacoustic microscopy for *in vivo* imaging of single capillaries. Opt Lett 2008;33(9):929–31.

Pereira de Vasconcelos A, Baldwin RA, Wasterlain CG. Nitric oxide mediates the increase in local cerebral blood flow during focal seizures (quantitative autoradiography/*N*-nitro-L-arginine/methylene blue/rat). Proc Natl Acad Sci 1995;92:3175–9.

Pinto KG, Scorza FA, Arida RM, Cavalheiro EA, Martins LD, Machado HR, et al. Sudden unexpected death in an adolescent with epilepsy: all roads lead to the heart? J Cardiol 2011;18(2):194–6.

Rajagopalan UM, Tanifuji M. Functional optical coherence tomography reveals localized layer-specific activations in cat primary visual cortex *in vivo*. Opt Lett 2007;32(17):2614–6.

Rao B, Yu L, Chiang HK, Zacharias LC, Kurtz RM, Kuppermann BD, et al. Imaging pulsatile retinal blood flow in human eye. J Biomed Opt 2008;13(4):040505.

Rao B, Li L, Maslov K, Wang LV. Hybrid-scanning optical-resolution photoacoustic microscopy for *in vivo* vasculature imaging. Opt Lett 2010a;35:1521–3.

Rao B, Li L, Maslov K, Wang LV. *In vivo*, dual-modality imaging of mouse eyes: optical coherence tomography and photoacoustic microscopy within a single instrument. Proc of SPIE 2010b;7550, 75501Q1–75501Q5.

Raol YH, Brooks-Kayal AR. Experimental models of seizures and epilepsies. Prog Mol Biol Transl Sci 2012;105:57–82.

Sato M, Nomura D, Tsunenari T, Nishidate I. In vivo rat brain measurements of changes in signal intensity depth profiles as a function of temperature using wide-field optical coherence tomography. Appl Opt 2010;49(30):20.

Santisakultarm TP, Schaffer CB. Optically quantified cerebral blood flow. J Cereb Blood Flow Metab 2011;31(6):1337–8.

Satomura Y, Seki J, Ooi Y, Yanagida T, Seiyama A. In vivo imaging of the rat cerebral microvessels with optical coherence tomography. Clin Hemorheol Microcirc 2004;31(1):31–40.

Schwartz TH, Chen LM, Friedman RM, Spencer DD, Roe AW. Intraoperative optical imaging of human face cortical topography: a case study. Neuroreport 2004;15(9):1527–31.

Schwartz TH, Bonhoeffer T. In vivo optical mapping of epileptic foci and surround inhibition in ferret cerebral cortex. Nat Med 2001;7(9):1063–7.

Tsytsarev V, Bernardelli C, Maslov KI. Living Brain Optical Imaging: Technology, Methods and Applications. J Neurosci Neuroeng 2012a;1(2):180–92.

Tsytsarev V, Maslov KI, Yao J, Parameswar AR, Demchenko AV, Wang LV. In vivo imaging of epileptic activity using 2-NBDG, a fluorescent deoxyglucose analog. J Neurosci Methods 2012b;203(1):136–40.

Tsytsarev V, Fukuyama H, Pope D, Pumbo E, Kimura M. Optical imaging of interaural time difference representation in rat auditory cortex. Front Neuroeng 2009;2(2).

Tsytsarev V, Pope D, Pumbo E, Yablonskii A, Hofmann M. Study of the cortical representation of whisker directional deflection using voltage-sensitive dye optical imaging. Neuroimage 2010;53(1):233–8.

Tsytsarev V, Premachandra K, Takeshita D, Bahar S. Imaging cortical electrical stimulation *in vivo*: fast intrinsic optical signal versus voltage-sensitive dyes. Opt Lett 2008;33(9):1032–4.

Tsytsarev V, Hu S, Yao J, Maslov KI, Barbour DL, Wang LV. Photoacoustic microscopy of microvascular responses to cortical electrical stimulation. J Biomed Opt 2011;16(7):076002.

Wang LV. Prospects of photoacoustic tomography. Med Phys 2008;35(12):5758–67.

Wang LV. Multiscale photoacoustic microscopy and computed tomography. Nature Photon 2009;3:503–9.

Wang LV, Hu S. Photoacoustic tomography: *in vivo* imaging from organelles to organs. Science 2012;335:1458–62.

Wang XD, Pang YJ, Ku G, Xie XY, Stoica G, Wang LV. Noninvasive laser-induced photoacoustic tomography for structural and functional *in vivo* imaging of the brain. Nat Biotechnol 2003;21(7):803–6.

Yao J, Xia J, Maslov KI, Nasiriavanaki M, Tsytsarev V, Demchenko AV, et al. Noninvasive photoacoustic computed tomography of mouse brain metabolism *in vivo*. Neuroimage 2012;1(64):257–66.

Zhao M, Nguyen J, Ma H, Nishimura N, Schaffer CB, Schwartz TH, et al. Preictal and ictal metabolic coupling surrounding a seizure focus. J Neurosci 2011;31(37):13292–300.